Dual superconductivity in the SU(2) pure gauge vacuum: A lattice study

Paolo Cea*
Dipartimento di Fisica dell'Università di Bari, 70126 Bari, Italy
and Istituto Nazionale di Fisica Nucleare, Sezione di Bari, 70126 Bari, Italy

Leonardo Cosmai†
Istituto Nazionale di Fisica Nucleare, Sezione di Bari, 70126 Bari, Italy
(Received 20 April 1995)

We investigate the dual superconductivity hypothesis in pure SU(2) lattice gauge theory. We focus on the dual Meissner effect by analyzing the distribution of the color fields due to a static quark-antiquark pair. We find evidence of the dual Meissner effect both in the maximally Abelian gauge and without gauge fixing. We measure the London penetration length. Our results suggest that the London penetration length is a physical gauge-invariant quantity. We put out a simple relation between the penetration length and the square root of the string tension. We find that our estimation is quite close to the extrapolated continuum limit available in the literature. A remarkable consequence of our study is that an effective Abelian theory can account for the long range properties of the SU(2) confining vacuum.

PACS number(s): 11.15.Ha

I. INTRODUCTION

Understanding the mechanism of quark confinement is a central problem in high-energy physics. This requires us, among other things, to identify the dynamical variables, which are relevant to confinement.

A satisfying solution would be to set up an approximate vacuum state, which confines color charges. This way one could derive an effective action, which describes the long-distance properties of QCD [1]. Even this incomplete program, however, mandates a nonperturbative approach. Fortunately we have at our disposal a framework in which we can do nonperturbative calculations, namely, the lattice discretization of gauge theories. Since a typical Monte Carlo simulation generates vacuum configurations, one expects to gain information on the nonperturbative vacuum structure.

However, a guideless search into the numerical configurations generated during Monte Carlo runs is hopeless. In other words, we need some theoretical input that selects the dynamical variables relevant to the confinement. The situation looks similar to the theory of superconductivity. Indeed, it was Cooper's observation that the Fermi surface is unstable with regard to the formation of bounded electron pairs that led Bardeen, Cooper, and Schrieffer to formulate the successful BCS superconductivity theory [2].

An interesting possibility was conjectured a long time ago by 't Hooft [3] and Mandelstam [4]. These authors proposed that the confining vacuum behaves as a coherent state of color magnetic monopoles. This is equivalent to saying that the vacuum is a magnetic (dual) superconductor. This fascinating proposal offers a picture of confinement whose physics can be clearly extracted. As a matter of fact, the dual Meissner effect causes the formation of chromoelectric flux tubes between chromoelectric charges leading to a linear rising potential. It is worthwhile to discuss briefly 't Hooft's proposal [5].

Let us consider the non-Abelian gauge theory spontaneously broken via the Higgs mechanism. The Higgs fields are in the adjoint representation. For concreteness we focus on the Georgi-Glashow model [6]. It is well known that the Georgi-Glashow model allows field configurations that correspond to magnetic monopoles [7]. Moreover, one readily finds that the monopole mass is given by

$$M_{\rm mon} = C\,\frac{M_W}{\alpha}\,, \tag{1.1}$$

where M_W is the mass of the charged vector boson, C a constant, and α the fine-structure constant. The dual superconductor scenario is realized if these magnetic monopoles condense by means of the magnetic Higgs mechanism. This means that the monopoles become tachyonic:

$$M^2_{\rm mon} \leq 0. \tag{1.2}$$

From Eq. (1.1) we see that $M^2_W \to 0$ (if we kept α fixed). The fact that M^2_W must go through zero suggests that the original Higgs field could be removed. Thus we are led to consider the pure gauge theory without elementary Higgs fields. The role of the scalar Higgs field is played by any operator that transforms in the adjoint representation of the gauge group. More precisely, after choosing an operator $X(x)$, which transforms according

*Electronic address: cea@bari.infn.it
†Electronic address: cosmai@bari.infn.it

to the adjoint representation, one fixes the gauge by diagonalizing $X(x)$ at each point. This choice does not fix the gauge completely; it leaves as residual invariance group the maximally Abelian (Cartan) subgroup of the gauge group. Such a procedure is known as Abelian projection [8]. For instance, if the gauge group is SU(N), then after gauge fixing the residual invariance group is $U(1)^{N-1}$. The world line of the monopoles can be identified as the lines where two eigenvalues of the operator $X(x)$ are equal. The dual superconductor idea is realized if these Abelian monopoles condense.

It is evident that the monopoles are dynamical; they will take part in the dynamics of the system. As a consequence the problem of monopole condensation cannot be dealt with the perturbation theory. On the other hand, the Abelian projection can be implemented on the lattice [9]. Thus, one can analyze the dynamics of the Abelian projected gauge fields by means of Monte Carlo simulations. In the following we shall consider the pure SU(2) gauge theory.

To perform the Abelian projection we make a choice for $X(x)$. The simpler possibility is to consider a local quantity. For instance, we can use a plaquette with a definite orientation (field-strength gauge) or the Polyakov loop (Polyakov gauge). In these unitary gauges we implement the gauge fixing by means of the matrices $V(x)$, which diagonalize $X(x)$ at each lattice site:

$$V(x)X(x)V^{\dagger}(x) = \mathrm{diag}\left[e^{i\alpha(x)}, e^{-i\alpha(x)}\right]. \tag{1.3}$$

It is straightforward to check that the residual gauge-invariance group is the U(1) group with transformations $\exp[i\sigma_3\theta(x)]$.

The Abelian projection of the gauge-transformed links

$$\widetilde{U}_{\mu}(x) = V(x)U_{\mu}(x)V^{\dagger}(x+\hat{\mu}) \tag{1.4}$$

amounts to writing

$$\widetilde{U}_{\mu}(x) = W_{\mu}(x)U^{A}_{\mu}(x) \tag{1.5}$$

with

$$U^{A}_{\mu}(x) = \mathrm{diag}\left[e^{i\theta^{A}_{\mu}(x)}, e^{-i\theta^{A}_{\mu}(x)}\right], \tag{1.6}$$

$$\theta^{A}_{\mu}(x) = \arg\left[\widetilde{U}_{\mu}(x)\right]_{11}. \tag{1.7}$$

$U^{A}_{\mu}(x)$ is the Abelian projection of $\widetilde{U}_{\mu}(x)$.

A different class of gauge fixing has been proposed in the literature: namely, the Abelian covariant gauge or maximally Abelian gauge [9]. In the continuum the maximally Abelian gauge corresponds to imposing the constraints [10]

$$D_{\mu}A^{\pm}_{\mu}(x) = 0\ , \tag{1.8}$$

where $A^{\pm}_{\mu} = A^{1}_{\mu} \pm iA^{2}_{\mu}$, and D_{μ} is the A^{3}_{μ}-covariant derivative. On the lattice the constraints (1.8) can be implemented like the Landau gauge [11]. Indeed Eq. (1.8) corresponds on the lattice to diagonalizing [10,12]

$$X(x) = \sum_{\mu}\left\{U_{\mu}(x)\sigma_3 U^{\dagger}_{\mu}(x) + U^{\dagger}_{\mu}(x-\hat{\mu})\sigma_3 U_{\mu}(x-\hat{\mu})\right\}. \tag{1.9}$$

To do this it is enough to maximize iteratively the quantity

$$R = \sum_{x,\mu}\left[\sigma_3\widetilde{U}_{\mu}(x)\sigma_3\widetilde{U}^{\dagger}_{\mu}(x)\right], \tag{1.10}$$

where the $\widetilde{U}_{\mu}(x)$'s are the gauge-transformed links (1.4). We thereby obtain the matrices $V(x)$ and perform the Abelian projection of the links by Eqs. (1.4)–(1.7).

From the above discussion it is evident that the monopole dynamic does depend on the choice of the operator needed to fix the gauge. On the other hand, the confinement of color charges via monopole condensation can not depend on the gauge fixing. However, it is conceivable that the dual superconductor scenario could manifest with a judicious choice of $X(x)$. This outcome could arise from a gauge fixing, which freezes the degrees of freedom that are irrelevant to the confinement. We feel that the situation is similar to the time-honored BCS theory of superconductivity. Indeed in the BCS theory one deals with a reduced Hamiltonian, which breaks the electromagnetic gauge invariance. Nevertheless, the reduced BCS Hamiltonian offered the correct explanation of the Meissner effect. As a matter of fact, it was showed [13] that the collective states, which are essential to restoring the gauge invariance, do not contribute to the BCS calculation of the Meissner effect. In other words, the reduced BCS Hamiltonian, by retaining the degrees of freedom relevant to the superconductivity, gives a sensible answer even though it breaks the electromagnetic gauge invariance.

Interestingly enough, it turns out that, if one fixes the maximally Abelian gauge, the Abelian projected links seem to retain the information relevant to the confinement [14]. Thus, it is important to deepen the study of the dynamics of the Abelian projected fields in that particular gauge fixing.

The aim of the present paper is to analyze the fingerprint of the dual superconductor hypothesis: namely, the Meissner effect. To this end, we analyze the distribution of the color field due to static quark-antiquark pair in SU(2) lattice gauge theory in the maximally Abelian gauge. Moreover, we will study the gauge dependence of the London penetration length. A partial account of this paper has been published in Ref. [15].

The plan of the paper is as follows. In Sec. II we explore the field configurations produced by the quark-antiquark static pairs both in the case of Abelian projected links after the maximally Abelian gauge has been fixed and in the case of full SU(2) links. In Sec. III we analyze the transverse distribution of the longitudinal chromoelectric field. In Sec. IV we investigate the relation between the penetration length and the string tension. Our conclusions are relegated in Sec. V. The Appendix comprises several technical details on the maximally Abelian gauge fixing.

II. COLOR FIELDS

In this section we analyze the distribution of the color fields due to static quark-antiquark pairs. Following the authors of Ref. [16], we can measure the color fields by means of the correlation of a plaquette U_p with a Wilson loop W. The plaquette is connected to the Wilson loop by a Schwinger line L (see Fig. 1). Moving the plaquette U_p with respect to the Wilson loop one can scan the structure of the color fields. In a previous study [17] we found evidence of the dual Meissner effect in the maximally Abelian gauge. In particular, we measured the penetration depth of the flux tube chromoelectric field. However, in Ref. [17] we employed rather small lattices ($L = 12$). In this work we extend our previous study in two directions. First, we perform numerical simulations on a lattice whose size ranges from $L = 16$ up to 24. In addition, we investigate the gauge invariance of the penetration length. To do this we perform the numerical simulations both in the maximally Abelian gauge and without gauge fixing.

A. SU(2)

According to Ref. [16], one can explore the field configurations produced by the quark-antiquark pair by measuring the connected correlation function (Fig. 1)

$$\rho_W = \frac{\langle \mathrm{tr}\left(WLU_PL^\dagger\right)\rangle}{\langle \mathrm{tr}(W)\rangle} - \frac{1}{2}\frac{\langle \mathrm{tr}(U_P)\mathrm{tr}(W)\rangle}{\langle \mathrm{tr}(W)\rangle}\ , \qquad (2.1)$$

where $U_P = U_{\mu\nu}(x)$ is the plaquette in the (μ,ν) plane. Note that the correlation function (2.1) is sensitive to the field strength rather than to the square of the field strength [18]:

$$\rho_W \underset{a\to 0}{\sim} a^2 g\left[\langle F_{\mu\nu}\rangle_{q\bar{q}} - \langle F_{\mu\nu}\rangle_0\right]\ . \qquad (2.2)$$

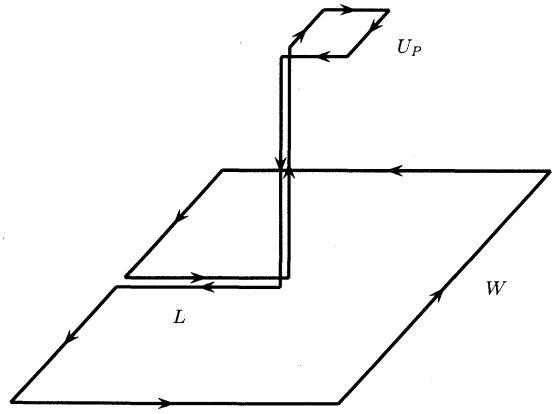

FIG. 1. The connected correlator (2.1) between the plaquette U_p and the Wilson loop. The subtraction appearing in the definition of correlator is not explicitly drawn.

According to Eq. (2.2) we define the color field strength tensor as

$$F_{\mu\nu}(x) = \frac{\sqrt{\beta}}{2}\rho_W(x)\ . \qquad (2.3)$$

By varying the distance and the orientation of the plaquette U_P with respect to the Wilson loop W, one can scan the color field distribution of the flux tube.

We performed numerical simulations with Wilson action and periodic boundary conditions using an overrelaxed Metropolis algorithm. Our data refer to 16^4, 20^4, and 24^4 lattices. To evaluate the correlator, Eq. (2.1), we used square Wilson loops $L_W \times L_W$, with $L_W = L/2 - 2$ (L being the lattice size), and rectangular Wilson loops $L/2 \times L/4$.

In order to reduce the quantum fluctuations we adopted the controlled cooling algorithm [19]. It is known [20] that by cooling equilibrium configurations in a smooth way, quantum fluctuations are reduced by a few orders of magnitude, while the string tension survives and shows a plateau. We shall show below that the penetration length behaves in a similar way.

For the reader's convenience let us, briefly, illustrate our cooling procedure. The lattice gauge configurations are cooled by replacing the matrix $U_\mu(x)$ associated with each link $l \equiv (x,\hat{\mu})$ with a new matrix $U'_\mu(x)$ in such a way that the local contribution to the lattice action

$$S(x) = 1 - \frac{1}{2}\mathrm{tr}\left\{U_\mu(x)k(x)F(x)\right\} \qquad (2.4)$$

is minimized. $\widetilde{F}(x) = k(x)F(x)$ is the sum over the "U staples" involving the link l and $k(x) = \sqrt{\det\left[\widetilde{F}(x)\right]}$, so that $F(x) \in \mathrm{SU}(2)$. In a "controlled" or "smooth" cooling step we have

$$U_\mu(x) \to U'_\mu(x) = V(x)U_\mu(x)\ , \qquad (2.5)$$

where $V(x)$ is the SU(2) matrix that maximizes

$$\mathrm{tr}\left\{V(x)U_\mu(x)F(x)\right\} \qquad (2.6)$$

subject to the following constraint on the SU(2) distance between $U_\mu(x)$ and $U'_\mu(x)$:

$$\frac{1}{4}\mathrm{tr}\left\{\left[U^\dagger_\mu(x) - U'^\dagger_\mu(x)\right]\left[U_\mu(x) - U'_\mu(x)\right]\right\} \le \delta^2\ . \qquad (2.7)$$

We adopt $\delta = 0.0354$. A complete cooling sweep consists in the replacement Eq. (2.5) at each lattice site. We do the above replacement vectorlike according to the standard checkerboard order.

The cooling technique allows us to disentangle the signal from the noise with a relatively small set of statistics. After discarding about 3000 sweeps to ensure thermalization, we collect measurements on configurations separated by 100 upgrades for nine different values of β in the range $2.45 \le \beta \le 2.7$. After cooling we obtained a good signal for ρ_W on very small statistical samples (20 – 100 configurations).

In Fig. 2 we report our results for the field strength

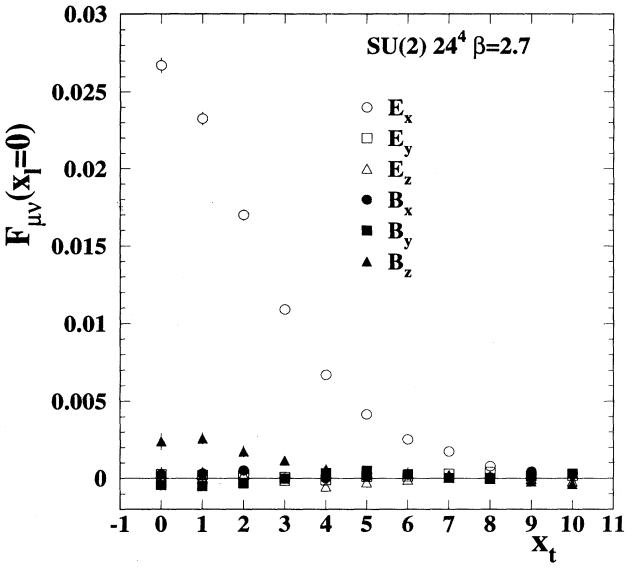

FIG. 2. The field strength tensor $F_{\mu\nu}(x_l, x_t)$ evaluated at $x_l = 0$ on a 24^4 lattice at $\beta = 2.7$, using Wilson loops of size 10×10 in Eq. (2.1).

tensor $F_{\mu\nu}(x_l, x_t)$, where the coordinates x_l, x_t measure, respectively, the distance from the middle point between quark and antiquark [which corresponds to the center of the spatial side of the Wilson loop W in Eq. (2.1)] and the distance out of the plane defined by the Wilson loop. The entries in Fig. 2 refer to measurements of the field strength tensor taken in the middle of the flux tube ($x_l = 0$) with eight cooling steps at $\beta = 2.7$ on the 24^4 lattice, using a square Wilson loop W of size 10×10. Our

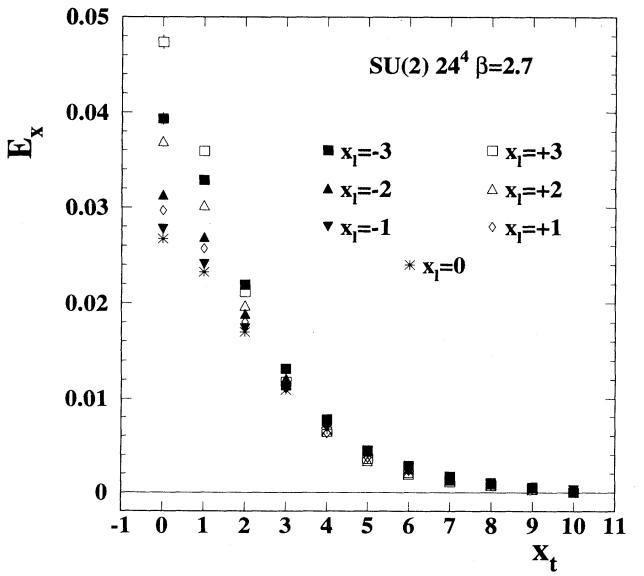

FIG. 3. The x_l dependence of the transverse profile of the longitudinal chromoelectric field $E_x(x_l, x_t) \equiv E_l(x_l, x_t)$.

results show that ρ_W is sizable when U_p and W are in parallel planes. This corresponds to measuring the component E_l of the chromoelectric field directed along the line joining the $q\bar{q}$ pair (E_x in Fig. 2). Moreover, we see that $E_l(x_l, x_t)$ decreases rapidly in the transverse direction x_t. In Fig. 3 we display the transverse distribution of the longitudinal chromoelectric field along the flux tube. The static color sources are at $x_l = +5$ and $x_l = -4$ (in lattice units). Figure 3 shows that the effects of the color sources on the chromoelectric fields extends over about three lattice spacings. Remarkably, far from the sources the longitudinal chromoelectric field is almost constant along the q-$\bar{q}$ line. Thus, the color field structure of the q-$\bar{q}$ tube, which emerges from our results, is quite simple: the flux tube is almost completely formed by the longitudinal chromoelectric field, which is constant along the flux tube (if x_l is not too close to the static color sources) and decreases rapidly in the transverse direction.

B. Maximally Abelian projection

In the 't Hooft formulation [8] the dual superconductor model is elaborated through the Abelian projection. The idea is that the Abelian projected gauge fields retain the long-distance physics of the gauge system. In particular, the physical quantities related to the confinement should be independent of the gauge fixing and agree with those obtained in the full gauge system. This suggested that we [17] investigate the Abelian projected correlator

$$\rho_W^A = \frac{\langle \mathrm{tr}\,(W^A U_P^A)\rangle}{\langle \mathrm{tr}\,(W^A)\rangle} - \frac{1}{2}\frac{\langle \mathrm{tr}\,(U_P^A)\,\mathrm{tr}\,(W^A)\rangle}{\langle \mathrm{tr}\,(W^A)\rangle} \,. \quad (2.8)$$

The correlator ρ_W^A is obtained from Eq. (2.1) with the substitution $U_\mu(x) \to U_\mu^A(x)$. For instance the Abelian projected plaquette in the (μ, ν) plane is

$$\begin{aligned} U_{\mu\nu}^A(x) &= U_\mu^A(x) U_\nu^A(x+\hat{\mu}) U_\mu^{A\dagger}(x+\hat{\nu}) U_\mu^{A\dagger}(x) \\ &= \mathrm{diag}\left\{\exp\left[i\theta_{\mu\nu}^A(x)\right], \exp\left[-i\theta_{\mu\nu}^A(x)\right]\right\} \,. \end{aligned} \quad (2.9)$$

Obviously the Abelian projected quantities are commutating, so we do not need the Schwinger lines in Eq. (2.8). It is worthwhile to stress that ρ_W^A is a gauge-dependent correlator. We performed measurements for six different values of β in the range $2.45 \le \beta \le 2.70$ using the 16^4 and 20^4 lattices. In this case we find a good signal without cooling. Measurements are taken on a sample of 500–700 configurations, each separated by 50 upgrades, after discarding 3000 sweeps to allow thermalization. The maximally Abelian gauge is fixed iteratively via the overrelaxation algorithm of Ref. [11] with the overrelaxation parameter $\omega = 1.7$ (for further details see the Appendix). Remarkably enough, it turns out that the Abelian field strength tensor

$$F_{\mu\nu}^A(x) = \frac{\sqrt{\beta}}{2}\rho_W^A(x) \quad (2.10)$$

behaves like the gauge-invariant one defined by Eq. (2.3). In Fig. 4 we report our results for the field strength ten-

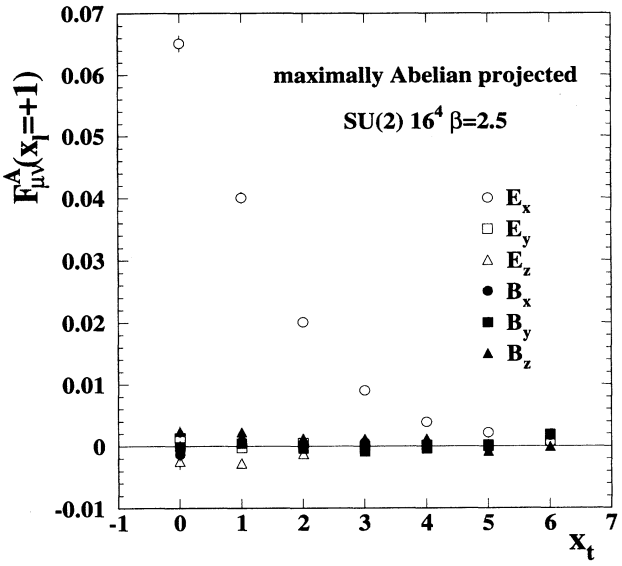

FIG. 4. The maximally Abelian projected field strength tensor $F^A_{\mu\nu}(x_l, x_t)$ evaluated at $x_l = +1$ on a 16^4 lattice at $\beta = 2.5$, using Wilson loops of size 6×6 in Eq. (2.8).

sor $F_{\mu\nu}(x_l, x_t)$ evaluated on maximally Abelian projected gauge configurations. The entries in Fig. 4 refer to measurements done at $x_l = +1$ on a 16^4 lattice at $\beta = 2.5$ using a square Wilson loop of size 6×6 in Eq. (2.8). Again we see that only the longitudinal chromoelectric field is sizable. In Fig. 5 we study the x_l dependence of the longitudinal Abelian chromoelectric field extracted using

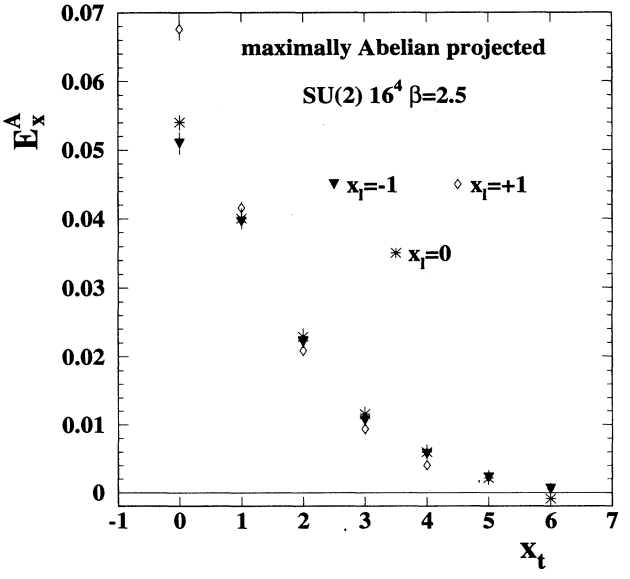

FIG. 5. The maximally Abelian projected longitudinal chromoelectric field $E^A_x(x_l, x_t) \equiv E^A_l(x_l, x_t)$ vs the transverse distance from the flux tube x_t for three different values of the longitudinal coordinate.

6×6 Wilson loop in Eq. (2.1) at $\beta = 2.5$ on the 16^4 lattice. Note that in the present case the static sources are at $x_l = +3$ and $x_l = -2$. The longitudinal Abelian chromoelectric field, and likewise the non-Abelian one, does not depend on the longitudinal coordinate x_l, far from the static sources. It is worthwhile observing that Fig. 5 suggests that the Abelian static sources are more localized than the non-Abelian ones. This is in accordance with our previous observation that the maximally Abelian gauge fixing seems to reduce the fluctuations, which are unimportant for the long-distance physics. In the next section we shall analyze our numerical data within the dual superconductor hypothesis.

III. LONDON PENETRATION LENGTH

A. SU(2)

If the dual superconductor scenario holds, the transverse shape of the longitudinal chromoelectric field E_l should resemble the dual version of the Abrikosov vortex field distribution. Hence we expect that $E_l(x_t)$ can be fitted according to

$$E_l(x_t) = \frac{\Phi}{2\pi}\mu^2 K_0(\mu x_t)\ , x_t > 0\ , \tag{3.1}$$

where K_0 is the modified Bessel function of order zero, Φ is the external flux, and $\lambda = 1/\mu$ is the London penetration length. Equation (3.1) is valid if $\lambda \gg \xi$, ξ being the coherence length (type-II superconductor). The length ξ measures the coherence of the magnetic monopole condensate (the dual version of the Cooper condensate). To determine the coherence length one should measure the correlation between the chromomagnetic monopoles. To do this one should construct a monopole creation operator. Unfortunately, thus far there is no convincing proposal for the monopole operator. However, recently a promising proposal has been advanced in Ref. [21]. We shall return to this matter in Sec. V. For the time being, because we are not able to determine the coherence length, we analyze our data far from the coherence region. To this end we try a fit with the transverse distribution (3.1) by discarding the points nearest to the flux tube ($x_t = 0$).

Let us discuss, firstly, the gauge-invariant correlator Eq. (2.1). We fit Eq. (3.1) to our data for $x_t \geq 2$ (in lattice units) obtaining $\chi^2/f \lesssim 1$ (we used the MINUIT code from the CERNLIB). In Fig. 6 we show $E_l(x_t)$ measured in the middle of the flux tube together with the result of our fit. The fit results in the two parameters Φ and μ. We have checked the stability of these parameters by fitting Eq. (3.1) to the data with the cuts $x_t \geq x_t^{\min}$, $x_t^{\min} = 2, 3, 4, 5$. In Table I we report the results of our stability analysis. We can see that within the statistical uncertainties the fit parameters are quite stable. So we are confident that our determination of the London penetration length is trustworthy. We ascertained, moreover, that the data obtained from the gauge-invariant correlator with cooled gauge configurations leads to a parameter

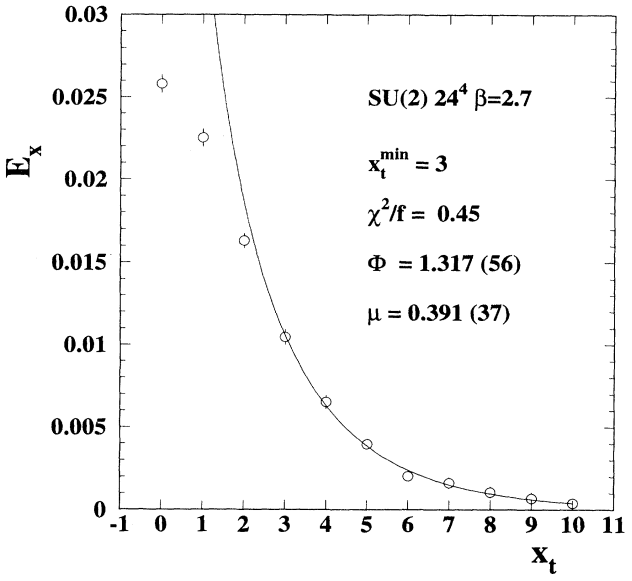

FIG. 6. The London fit (3.1) to the data for the longitudinal chromoelectric field.

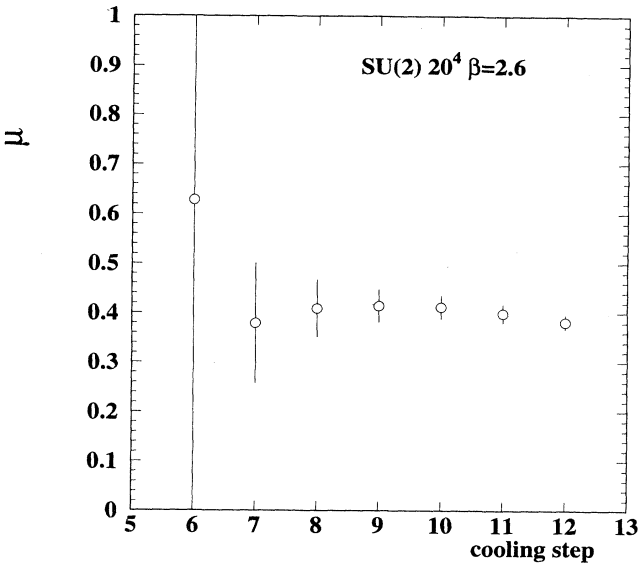

FIG. 7. The inverse of the penetration length μ vs the number of the cooling steps obtained by fitting the transverse profile of the longitudinal chromoelectric field at $x_l = 0$ (8×8 Wilson loop).

μ, which shows a plateau versus the number of cooling steps (see Fig. 7). This corroborates our expectation that the long range physics is unaffected by the cooling procedure. On the other hand, Fig. 8 indicates that the overall normalization of the transverse distribution of the longitudinal chromoelectric field is affected by the cooling. In fact the parameter Φ does not stay constant with the cooling. We feel that this is an indication that the flux Φ is strongly affected by lattice artefact. This point will be thoroughly discussed below.

In Figs. 9 and 10 we display the inverse of the penetration length μ (in units of $\Lambda_{\overline{\rm MS}}$, where $\overline{\rm MS}$ denotes the modified minimal subtraction scheme) and the external flux Φ versus β. These data are obtained by fitting Eq. (3.1) to the data extracted from square Wilson loops (open points) and rectangular Wilson loops (full points). A few comments are in order. A look at Fig. 9 shows that the inverse of the penetration length μ agrees within statistical fluctuations for both kinds of Wilson loops. However, we see that for $\beta \gtrsim 2.65$ the parameter μ arising from the rectangular Wilson loops seem to display sizable finite volume effects. On the other hand, we find that the parameter μ extracted from the square Wilson loops displays finite volume effects for $\beta > 2.7$, in the case of the 24^4 lattice. So in order to simulate in the range $\beta > 2.7$ we need lattices with $L > 24$.

Figure 9 suggests that the ratio $\mu/\Lambda_{\overline{\rm MS}}$ displays an approximate plateau in β. Indeed we fitted the ratio with a constant and obtained

TABLE I. Fit parameters in Eq. (3.1) vs the number of discarded points in the x_t direction.

	Fit parameters stability		
$x_t^{\rm min}$	Φ	μ	χ^2/f
1	1.413 45 (7599)	0.271 23 (1246)	10.041 40
2	1.297 05 (6052)	0.349 47 (2175)	1.179 81
3	1.316 56 (5568)	0.390 57 (3695)	0.452 13
4	1.357 80 (11 210)	0.411 92 (6162)	0.442 79
5	1.299 26 (26 320)	0.393 28 (10 050)	0.522 73

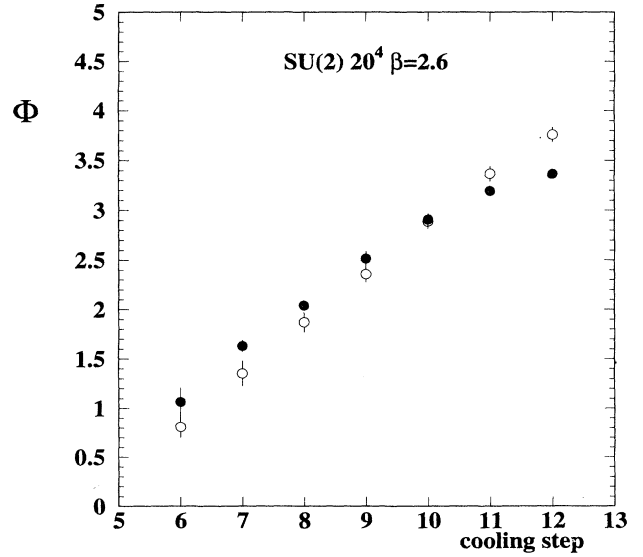

FIG. 8. The parameter Φ in Eq. (3.1) obtained by fitting the transverse profile of the longitudinal chromoelectric field at $x_l = 0$ vs the number of cooling steps. Open points refer to 8×8 Wilson loop and full points to 10×5 Wilson loop.

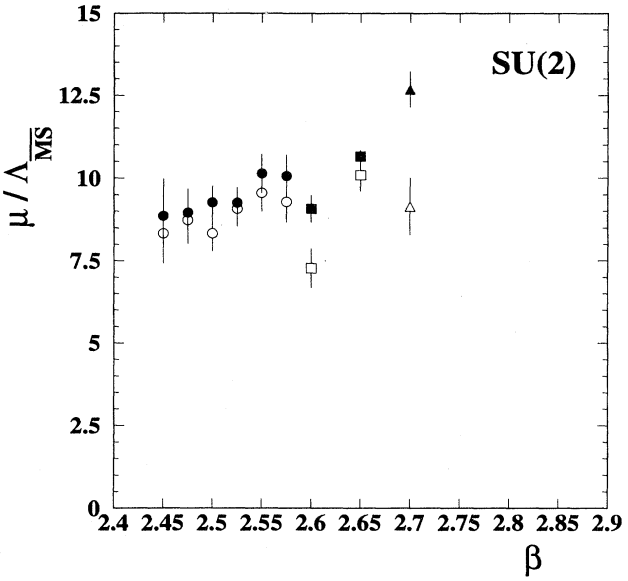

FIG. 9. $\mu/\Lambda_{\overline{\rm MS}}$ vs β. Full points correspond to rectangular Wilson loops and open points to square Wilson loops. Circles $L = 16$, squares $L = 20$, and triangles $L = 24$.

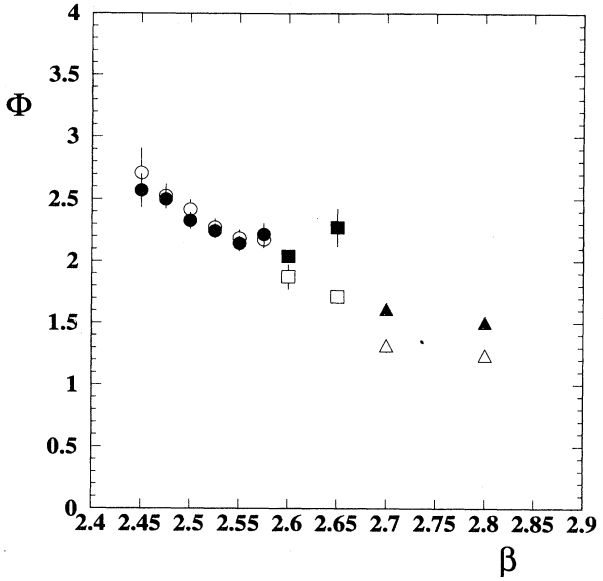

FIG. 10. Φ vs β. Symbols as in Fig. 9.

$$\frac{\mu}{\Lambda_{\overline{\rm MS}}} = 8.96(31)\,, \qquad \chi^2/f = 2.11 \tag{3.2}$$

using square Wilson loops in Eq. (2.1), and

$$\frac{\mu}{\Lambda_{\overline{\rm MS}}} = 9.36(29)\,, \qquad \chi^2/f = 0.53 \tag{3.3}$$

for rectangular Wilson loops (discarding in the fit the points at $\beta \geq 2.65$).

Equations (3.2) and (3.3) corroborate our previous observation on the consistency of the penetration length. By fitting all the data we obtain

$$\frac{\mu}{\Lambda_{\overline{\rm MS}}} = 9.17(21)\,, \qquad \chi^2/f = 1.48\,. \tag{3.4}$$

It is worthwhile to stress that our evidence for asymptotic scaling of the penetration length is only indicative. In general, it should be much easier to check scaling rather than asymptotic scaling. We looked at the scaling of μ extracted from square Wilson loops with the square root of the string tension (we have used the string tension extracted from large Wilson loops). We found that there is approximate scaling of μ with $\sqrt{\sigma}$ for $\beta \geq 2.5$:

$$\frac{\mu}{\sqrt{\sigma}} = 4.04(18)\,, \qquad \chi^2/f = 1.38\,. \tag{3.5}$$

So we see that our data on the penetration length are in agreement with the general expectation that scaling goes better than asymptotic scaling. On the other hand, the approximate evidence of asymptotic scaling is a natural consequence of the fact that the penetration length is a physical quantity related to the size D of the flux tube [17]:

$$D \simeq \frac{2}{\mu}\,. \tag{3.6}$$

As concerns the parameter Φ, Fig. 10 shows that Φ is rather insensitive to the shape of the Wilson loops used in Eq. (2.1) (again the data from rectangular Wilson loops are affected by finite volume effects for $\beta \gtrsim 2.65$). Moreover, Φ decreases rapidly by increasing β and seems to saturate to a value quite close to 1. We postpone the discussion of this behavior until the comparison with the results obtained using Abelian projected configurations in the maximally Abelian gauge.

B. Maximally Abelian projection

Let us consider, now, the Abelian projected field-strength tensor Eq. (2.10). As we saw, only the longitudinal Abelian chromoelectric field is sizable. As in the previous case, we try to fit the data with the law

$$E_l^A(x_t) = \frac{\Phi_A}{2\pi}\mu_A^2 K_0(\mu_A x_t)\,, \quad x_t > 0\,. \tag{3.7}$$

Again we find (see Fig. 11) that Eq. (3.7) reproduces our data quite well for $x_t \geq 2$ ($\chi^2/f \lesssim 1$). In Table II we check the stability of the fit parameters. In Fig. 12 we display the ratio $\mu_A/\Lambda_{\overline{\rm MS}}$ obtained by fitting Eq. (3.7) to the data in the case of square Wilson loops (open points) and rectangular Wilson loops (full points). Within the (rather large) statistical uncertainties, the parameter μ_A agrees for the two different Wilson loops. Moreover, the data suggest that the ratio $\mu_A/\Lambda_{\overline{\rm MS}}$ does not depend on β. Indeed we fit the ratio with a constant and find

$$\frac{\mu_A}{\Lambda_{\overline{\rm MS}}} = 8.26(67)\,, \qquad \chi^2/f = 0.41 \tag{3.8}$$

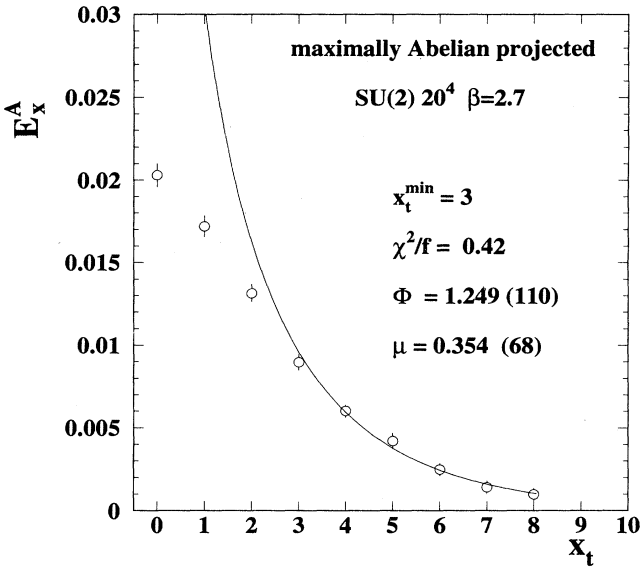

FIG. 11. London fit (3.7) to the data for the Abelian longitudinal chromoelectric field at $x_l = 0$ for square Wilson loop.

using square Wilson loops in Eq. (2.8), and

$$\frac{\mu_A}{\Lambda_{\overline{\rm MS}}} = 8.27(52)\,, \qquad \chi^2/f = 1.87 \tag{3.9}$$

for rectangular Wilson loops. An overall fit of all the data gives

$$\frac{\mu_A}{\Lambda_{\overline{\rm MS}}} = 8.27(41)\,, \qquad \chi^2/f = 1.05\,. \tag{3.10}$$

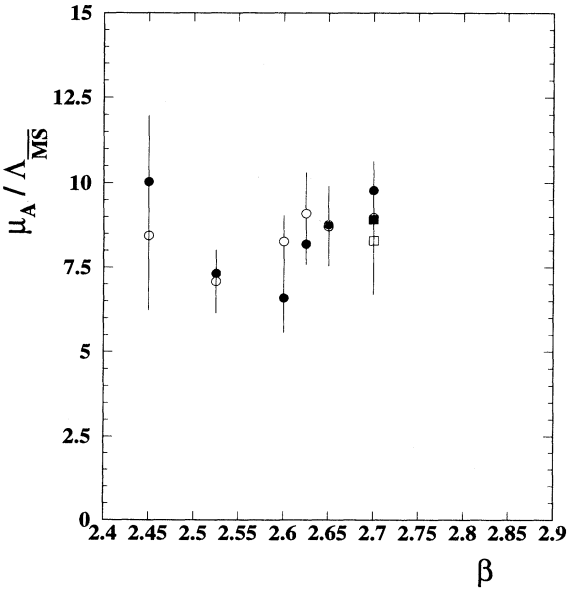

FIG. 12. $\mu_A/\Lambda_{\overline{\rm MS}}$ vs β. Full points correspond to rectangular Wilson loops and open points to square Wilson loops. Circles $L = 16$ and squares $L = 20$.

TABLE II. Fit parameters in Eq. (3.7) vs the number of discarded points in the x_t direction.

	Fit parameters stability		
$x_t^{\rm min}$	Φ_A	μ_A	χ^2/f
1	1.560 16 (21 253)	0.208 52 (2244)	4.351 99
2	1.287 96 (15 337)	0.283 66 (3880)	1.335 79
3	1.248 78 (10 988)	0.354 28 (6828)	0.418 57
4	1.342 01 (19 876)	0.419 71 (12 542)	0.173 80

Note that Eq. (3.2) and Eqs. (3.8)–(3.10) give consistent value for the ratio $\mu/\Lambda_{\overline{\rm MS}}$. On the other hand, the ratio $\mu/\Lambda_{\overline{\rm MS}}$, Eq. (3.3), extracted from the gauge-invariant correlator ρ_W with rectangular Wilson loops is slightly higher than Eqs. (3.8)–(3.10). Indeed, Eq. (3.3) and Eqs. (3.8)–(3.10) are consistent within two standard deviations. We feel that this small discrepancy is due to the fact that the rectangular Wilson loops seem to be more sensitive to finite volume effects. For this reason we shall, henceforth, refer to the data extracted from square Wilson loops.

In Fig. 13 we report the ratio $\mu/\Lambda_{\overline{\rm MS}}$ and $\mu_A/\Lambda_{\overline{\rm MS}}$ versus β obtained by the data corresponding to square Wilson loops. We can see that the London penetration length extracted from the gauge-invariant correlator Eq. (2.1) agrees with the one extracted from the Abelian projected correlator Eq. (2.8). In Fig. 13 we show also the result obtained by fitting together the data (for square Wilson loops):

$$\frac{\mu}{\Lambda_{\overline{\rm MS}}} = 8.84(28)\,, \qquad \chi^2/f = 1.44\,. \tag{3.11}$$

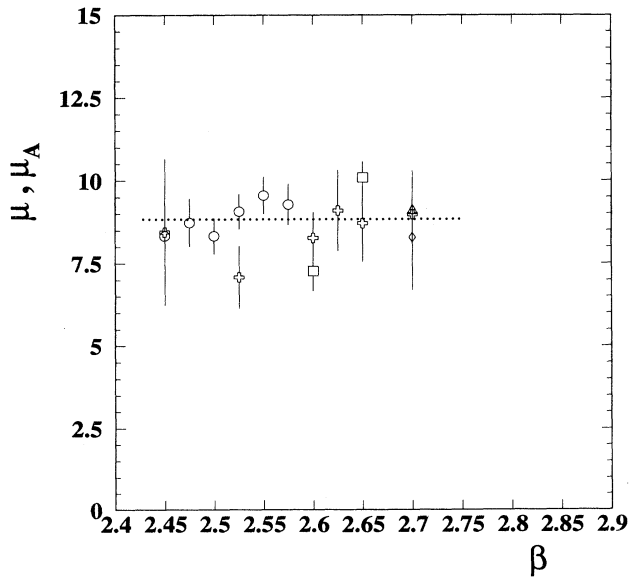

FIG. 13. μ and μ_A (in units of $\Lambda_{\overline{\rm MS}}$) vs β for square Wilson loops. Circles, squares, and the triangle refer to $L = 16$ 20, and 24, respectively. Crosses and the diamond refer to the Abelian projected correlator ρ_W^A with $L = 16$ and 20, respectively.

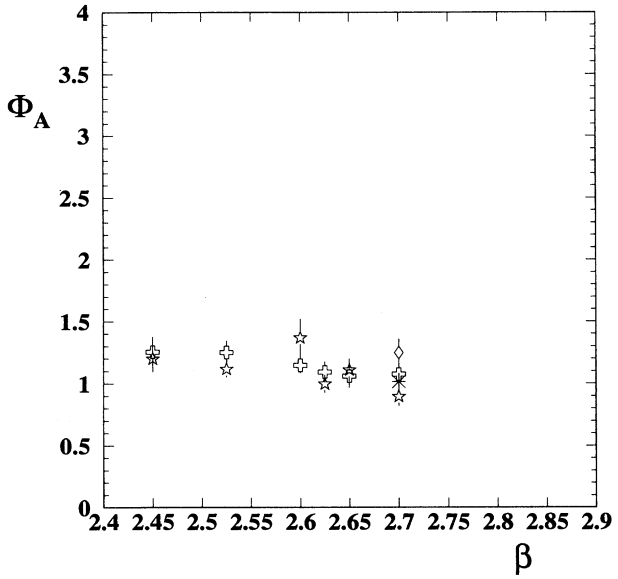

FIG. 14. Φ_A vs β. Crosses and the diamond correspond to square Wilson loops with $L = 16$ and 20, respectively; stars and the asterisk correspond to a rectangular Wilson loop with $L = 16$ and 20, respectively.

As a consequence, we can safely affirm that the London penetration length is gauge invariant. We feel that this result strongly supports the dual superconductor mechanism of confinement.

As concerns the parameter Φ_A, we find that, unlike the previous case, Φ_A does not depend strongly on β (see Fig. 14). Moreover, we see that Φ_A is quite close to 1. It is worthwhile discussing the physical interpretation of Φ. The total flux Φ_T of the flux tube chromoelectric field is given by

$$\Phi_T = \int d^2x_t E_l(x_t) \,, \tag{3.12}$$

where the integral extends over a plane transverse to the line joining the static color charges. As we have already discussed, the transverse distribution of the longitudinal chromoelectric field can be described by the law Eq. (3.1) when $x_t > 0$. Obviously we cannot extend the validity of Eq. (3.1) up to $x_t \to 0$. Indeed for $x_t \to 0$ we encounter a logarithmic divergence in K_0. On the other hand, $E_l(x_t)$ is finite in the coherence region $x_t \lesssim \xi$. However, if $\lambda/\xi \gtrsim 1$, we estimate that the extrapolation up to the origin introduces an overestimation of the integral (3.12) by less than 10%. So, inserting (3.1) into (3.12), we get

$$\Phi_T = \int d^2x_t E_l(x_t) \simeq \Phi \,. \tag{3.13}$$

Equations (3.12) and (3.13) tell us that the parameter Φ measures the total flux if $\lambda/\xi \gg 1$. In U(1) it turns out that $\Phi = 1$, since that happens to be one unit of quantized electric flux [22]. If the dynamics of the Abelian projected fields resembles the gauge fields of U(1), then we expect that $\Phi_A \simeq 1$. Indeed we find (square Wilson loops)

$$\Phi_A = 1.15(5) \,, \qquad \chi^2/f = 0.79 \,. \tag{3.14}$$

From the previous discussion it follows that Eq. (3.14) seems to indicate that $\lambda/\xi \sim 1$.

We would like to contrast Eq. (3.14) with the behavior of Φ. In Fig. 15 we report Φ_A and Φ versus β. The behavior of Φ under the cooling (see Fig. 8) suggested that the external flux is strongly affected by lattice artefacts. Moreover, Fig. 15 indicates that the lattice artefacts seem to disappear by increasing β. Thus, we are led to suspect that the external flux gets renormalized by irrelevant operators, whose effects are strongly suppressed in the maximally Abelian gauge.

IV. STRING TENSION

In the preceding section we have shown that the color fields of a static quark-antiquark pair are almost completely described by the longitudinal chromoelectric field. Moreover, we showed that the longitudinal chromoelectric field is almost constant along the flux tube. This means that the long-distance potential, which feels the color charges, is linear. Obviously the string tension is given by the energy stored into the flux tube per unit length. As a consequence we can write

$$\sigma \simeq \frac{1}{2} \int d^2x_t E_l^2(x_l, x_t) \,. \tag{4.1}$$

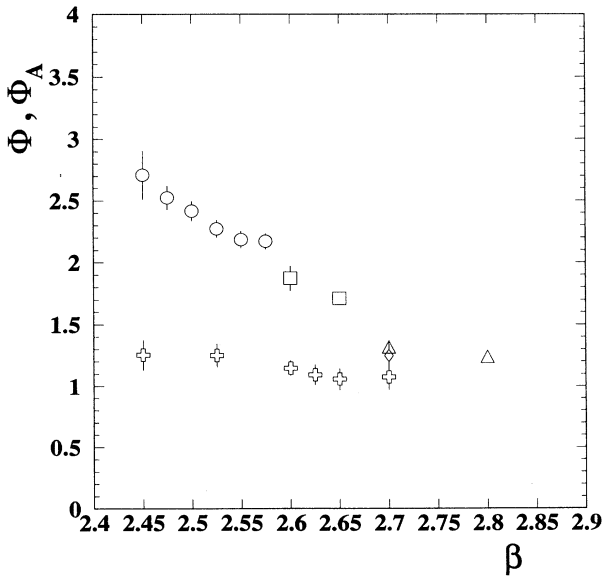

FIG. 15. Φ and Φ_A vs β for square Wilson loops. Points and crosses refer to $L = 16$, squares and the diamond to $L = 20$, and triangles to $L = 24$. Crosses and the diamond correspond to the maximally Abelian gauge.

We stress that the string tension σ defined by Eq. (4.1) does not depend on x_l as long as the longitudinal chromoelectric field is constant along the flux tube. As we have already discussed, working on a finite lattice results in the limitations $x_l = 0, \pm 1$ (in lattice units) in the integrand in Eq. (4.1). Keeping these limitations in mind, from Eq. (4.1) we can obtain an explicit relation between the string tension and the parameters Φ and μ. Indeed, if we extrapolate Eq. (3.1) up to $x_t = 0$, by using

$$\int_0^\infty dx\, x K_0^2(x) = \frac{1}{2}\,, \tag{4.2}$$

we get

$$\sqrt{\sigma} \simeq \frac{\Phi}{\sqrt{8\pi}}\mu\,. \tag{4.3}$$

The main uncertainty in Eq. (4.3) comes out from the parameter Φ. As explained in Secs. II and III, we computed the parameters Φ and μ on SU(2) gauge configurations and on the maximally Abelian projected gauge configurations. In the latter case, $\Phi_A \approx 1$ and is independent of β. On the other hand, for SU(2), $\Phi > 1$, and it approaches values very close to Φ_A by increasing β. As we have already discussed, we feel that the external flux Φ is strongly affected by lattice artefacts. We can try to get rid of these effects by assuming that, in the limit $\beta \to \infty$,

$$\Phi \simeq \Phi_A \simeq 1\,. \tag{4.4}$$

In this way Eq. (4.3) becomes

$$\sqrt{\sigma} \simeq \frac{\mu}{\sqrt{8\pi}}\,. \tag{4.5}$$

A striking consequence of Eq. (4.5) is that, due to $\mu \simeq \mu_A$,

$$\sqrt{\sigma} \simeq \sqrt{\sigma}_A\,, \tag{4.6}$$

within statistical uncertainties.

In Fig. 16 we report Eq. (4.5) in units of $\Lambda_{\overline{\rm MS}}$ versus $a\Lambda_{\overline{\rm MS}}$. Fitting the data all together to a constant, we get (square Wilson loops)

$$\frac{\sqrt{\sigma}}{\Lambda_{\overline{\rm MS}}} = 1.76(6)\,, \qquad \chi^2/f = 1.44\,. \tag{4.7}$$

The quoted error in Eq. (4.7) is purely statistical. However, one should keep in mind that our theoretical uncertainties in the estimation of the string tension (4.7) introduce a systematic error that can be of the order of 10%. Nevertheless, it is gratifying to see that our estimation of the string tension Eq. (4.7) is consistent with (star in Fig. 16)

$$\frac{\sqrt{\sigma}}{\Lambda_{\overline{\rm MS}}} = 1.79(12)\,. \tag{4.8}$$

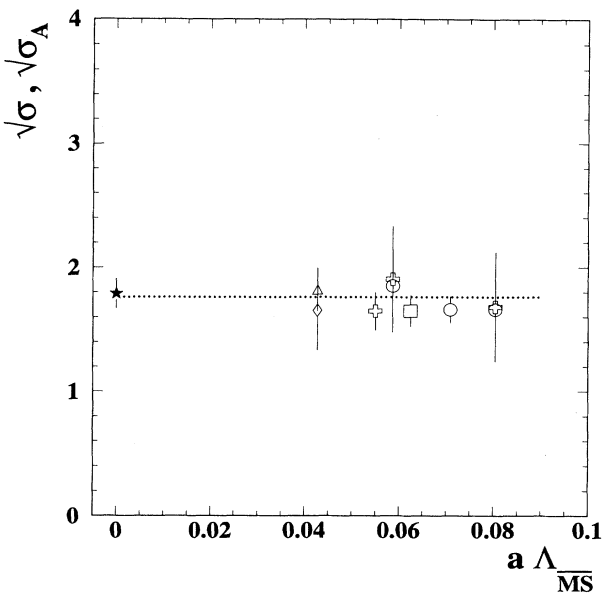

FIG. 16. String tension (in units of $\Lambda_{\overline{\rm MS}}$) evaluated through Eq. (4.1). The star refers to the value given in Ref. [23]. Symbols are as in Fig. 15. For figure readability, not all the available data are displayed.

The value quoted in Eq. (4.8) was obtained in Ref. [23] by the linear asymptotic extrapolation of the string tension data extracted from Wilson loops on lattices larger than ours.

V. CONCLUSIONS

Let us conclude by stressing the main results of this paper. We investigated the color field strength tensor of the q-$\bar{q}$ flux tube by means of the connected correlators (2.1) [full SU(2)] and (2.8) (maximally Abelian gauge).

The main advantage of using the connected correlator (2.1) and (2.8) resides in the fact that the connected correlators are sensitive to the field strength rather than to the square of the field strength. As a consequence, we are able to detect a sizable signal even with relatively low statistics. It turns out that the flux tube color fields are composed by the chromoelectric component parallel to the line joining the static charges. Moreover the longitudinal chromoelectric field is almost constant far from the color sources, and it decreases rapidly in the directions transverse to the line connecting the charges. As a matter of fact, we found that the transverse distribution of the longitudinal chromoelectric field behaves in accord with the dual Meissner effect. This allows us to determine the London penetration length. We checked that the penetration length is a physical gauge-invariant quantity. A remarkable consequence of our findings is that the long range properties of the SU(2) confining vacuum can be

described by an effective Abelian theory. In addition, after fixing the gauge with the constraints (1.8)–(1.10), it seems that the degrees of freedom that are not relevant to the confinement get suppressed.

Finally, we put out a very simple relation between the string tension and the penetration length, which gives an estimate of $\sqrt{\sigma}$ quite close to the extrapolated continuum limit available in the literature.

In conclusion, we would like to stress that the most urgent problem to be addressed in future studies is the reliable estimation of the coherence length ξ. The results in Sec. III give an indirect and, admittedly, very weak indication that $\lambda/\xi \sim 1$. As we have already discussed, the coherence length is determined by the monopole condensate, the order parameter for the confinement. Recently two different groups [24,25] gave an estimation of the coherence length. These authors calculated the electric flux and magnetic monopole current distribution in the presence of a static quark-antiquark pair for the SU(2) lattice gauge theory in the maximally Abelian gauge. The magnetic monopoles are identified using the DeGrand-Toussaint [26] construction. By using a dual form of the Ginzburg-Landau theory [27], which allows the magnitude of the monopole condensate density to vary in space, they fitted the data and obtain λ/a and ξ/a. They found that the coherence length is comparable to the penetration length. Even though we feel that the approach of Refs. [24,25] is interesting, we would like to observe that it relies heavily on the definition of the magnetic monopole current. As a matter of fact, in Ref. [28] it was pointed out that the DeGrand-Toussaint definition of the monopole density is plagued by lattice artefacts, which are, however, less severe in the maximally Abelian gauge. So the DeGrand-Toussaint monopole density is not an order parameter for confinement. Thus, the approach of Refs. [24,25] is plagued by the ambiguities related to the definition of the monopole current. On the other hand, in our approach we work outside the coherence region, so we feel that our results do not manifest the above-mentioned problem. To clarify this point, the study of the distribution of color fields in the presence of a static quark-antiquark pair in the framework of the dual Ginzburg-Landau model with the magnetic monopole current constructed by means of the monopole creation operator proposed in Ref. [21] should be of great help.

APPENDIX

In this appendix we give more details on the algorithm used to fix the maximally Abelian gauge. On the lattice, the maximally Abelian gauge is obtained by maximizing the lattice functional

$$R_l = \sum_{x,\hat{\mu}} \frac{1}{2}\mathrm{tr}\left[\sigma_3 U_\mu(x)\sigma_3 U_\mu^\dagger(x)\right] \tag{A1}$$

over all SU(2) gauge transformations

$$U_\mu(x) \to \widetilde{U}_\mu(x) = g(x)U_\mu(x)g^\dagger(x)\ , \tag{A2}$$

where $g(x) \in \mathrm{SU}(2)$. Under an arbitrary gauge transformation the variation of the lattice functional Eq. (A1) is

$$\Delta R_l(x) = \frac{1}{2}\mathrm{tr}\left[g^\dagger(x)\sigma_3 g(x)X(x)\right] - \frac{1}{2}\mathrm{tr}\left[\sigma_3 X(x)\right]\ , \tag{A3}$$

where

$$X(x) = \sum_\mu \left[U_\mu(x)\sigma_3 U_\mu^\dagger(x) + U_\mu^\dagger(x-\hat{\mu})\sigma_3 U_\mu(x-\hat{\mu})\right] \tag{A4}$$

belongs to the SU(2) algebra. If we have locally maximized the lattice functional (A1) with respect to an arbitrary gauge transformation, then we have

$$\Delta R_l(x) = 0\ . \tag{A5}$$

From Eq. (A3) it follows that

$$X(x) = g(x)X(x)g^\dagger(x)\ ; \tag{A6}$$

i.e., $X(x)$ must be diagonal. So that maximizing $R_l(x)$ is equivalent to diagonalizing the Hermitian matrix $X(x)$. Note that maximization of $R_l(x)$ at the given lattice site x is accomplished by a gauge transformation $g(x)$, which, in turn, affects the value of the local operator $X(x)$ at the nearest neighbors. Therefore, the maximization of the lattice functional (A1) can be achieved only by an iterative procedure over the whole lattice. In an equivalent manner one can find $g(x)$ as the matrix that diagonalizes $X(x)$ or as the matrix that maximizes $R_l(x)$.

To obtain explicitly the gauge element $g(x)$, which maximizes $R_l(x)$, let us write $R_l(x)$ as

$$\begin{aligned} R_l(x) &= \frac{1}{2}\mathrm{tr}\left[\sigma_3 g^\dagger(x)\sigma_3 g(x)X(x)\sigma_3\right] \\ &= k(x)\frac{1}{2}\mathrm{tr}\left[\sigma_3 g^\dagger(x)\sigma_3 g(x)V(x)\right]\ , \end{aligned} \tag{A7}$$

where

$$V(x) = \frac{X(x)\sigma_3}{k(x)}\ , \qquad k(x) = \sqrt{\det\left[X(x)\sigma_3\right]}\ , \tag{A8}$$

ensuring that $V(x)$ is an element of SU(2). As one can easily recognize from Eq. (A4),

$$V(x) = v_0(x) + i[v_1(x)\sigma_1 + v_2(x)\sigma_2]\,. \tag{A9}$$

Note that the term proportional to σ_3 is absent. Now, we observe that, if we consider $\widetilde{g}(x) = u(x)g(x)$ [with $u(x) = u_0(x) + iu_3(x)\sigma_3$] instead of $g(x)$, then Eq. (A7) is invariant. So we can assume without loss of generality that in Eq. (A7) $g(x) = g_0(x) + i[g_1(x)\sigma_1 + g_2(x)\sigma_2]$. As a consequence, Eq. (A7) is maximized when

$$g_0(x) = \pm\sqrt{\frac{v_0(x)+1}{2}}\,,$$
$$g_1(x) = -\frac{v_1(x)}{2g_0(x)}\,,$$
$$g_2(x) = -\frac{v_2(x)}{2g_0(x)}\,. \qquad \text{(A10)}$$

Since maximization of (A1) results in an iterative procedure, we must have at our disposal a convergence criterion. To have a measure of the goodness of gauge fixing, we consider the average size of the nondiagonal matrix elements of X over the whole lattice:

$$\left\langle \left|X^{\rm nd}\right|^2 \right\rangle = \frac{1}{L^4}\sum_x \left[|X_1|^2 + |X_2|^2\right]\,, \qquad \text{(A11)}$$

where $X = X_1\sigma_1 + X_1\sigma_2 + X_1\sigma_3$. We stop the iterations when

$$\left\langle \left|X^{\rm nd}\right|^2 \right\rangle \le D\,, \qquad \text{(A12)}$$

where D is some (small) positive number. In our simulation we used $D = 10^{-6}$.

In order to accelerate the convergence of the algorithm, we adopted the overrelaxation method [29] suggested in Ref. [11]. Once we have found the matrix $g(x)$, which maximizes (A3), we make the substitution

$$g(x) \to g_{\rm over}(x) = g(x)^\omega\,, \qquad \text{(A13)}$$

where the overrelaxation parameter ω varies in the interval $1 \le \omega \le 2$. The exponentiation in Eq. (A13) is obtained through the following representation for an element $u \in {\rm SU}(2)$:

$$u = \cos\left(\frac{r}{2}\right) + i\,(\vec{\sigma}\cdot\hat{r})\sin\left(\frac{r}{2}\right)\,, \qquad \text{(A14)}$$

where $\hat{r} = \vec{r}/|\vec{r}|$, $r = |\vec{r}|$.

In our Monte Carlo runs we used $\omega = 1.7$. However, we would like to stress that [11] an optimal overrelaxation parameter ω_c exists. Moreover, for large lattice size L it is believed that

$$\omega_c = \frac{2}{1+\frac{c}{L}}\,, \qquad \text{(A15)}$$

where the constant c is problem dependent. As a matter of fact, it turns out that a better convergence can be obtained using values of ω close to 1.9 (see Fig. 17). Indeed we obtained $\omega_c \simeq 1.92$ for $L = 16$. Inserting this value into Eq. (A15), we find $c \simeq 0.7$. It is remarkable that our value for the constant c agrees with the one relevant to the Landau gauge fixing [11].

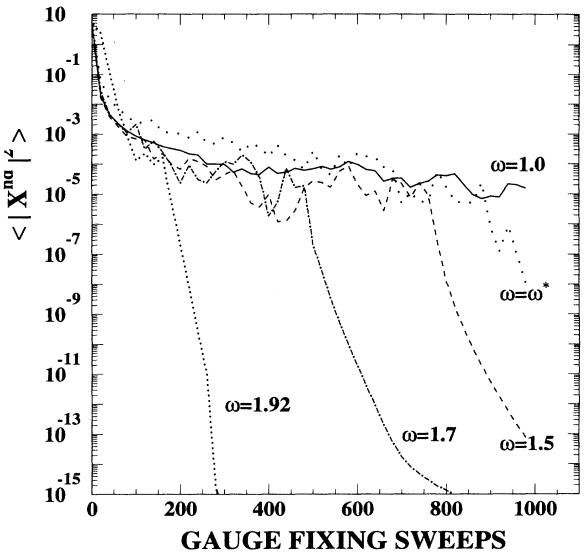

FIG. 17. Efficacy of gauge fixing defined by Eq. (A11) as a function of the overrelaxation parameter ω for the $L = 16$ lattice. The case $\omega = \omega^*$ corresponds to alternate $\omega = 1.0$ with $\omega = 2.0$ in the gauge-fixing sweeps.

[1] M. Baker, S. James, and F. Zachariasen, Phys. Rep. **209**, 73 (1991).
[2] For a historical overview, see J. R. Schrieffer, Physics Today **45** (4), 46 (1992).
[3] G. 't Hooft, in *High Energy Physics*, Proceedings of the EPS International Conference, Palermo, Italy, 1975, edited by A. Zichichi (Editrice Compositori, Bologna, 1976); Phys. Scr. **25**, 133 (1982).
[4] S. Mandelstam, Phys. Rep. **23C**, 245 (1976).
[5] This point is thoroughly discussed in the second paper in Ref. [3].
[6] H. Georgi and S. L. Glashow, Phys. Rev. Lett. **28**, 1494 (1972).
[7] A. M. Polyakov, JETP Lett. **20**, 194 (1974); G. 't Hooft, Nucl. Phys. **B79**, 276 (1974).
[8] G. 't Hooft, Nucl. Phys. **B190**, 455 (1981).
[9] A. S. Kronfeld, M. L. Laursen, G. Schierholz, and U.-J. Wiese, Phys. Lett. B **198**, 516 (1987); A. S. Kronfeld, M. L. Laursen, G. Schierholz, and U.-J. Wiese, Nucl. Phys. **B293**, 461 (1987).
[10] A. van der Sijs, Ph.D. thesis, Amsterdam University 1991; J. Smit and A. van der Sijs, Nucl. Phys. **B355**, 603 (1991).
[11] J. E. Mandula and M. Ogilvie, Phys. Lett. B **248**, 156 (1990).
[12] T. Suzuki and I. Yotsuyanagi, Phys. Rev. D **42**, 4257 (1990).
[13] P. W. Anderson, Phys. Rev. **110**, 827 (1958); Y. Nambu, *ibid.* **117**, 648 (1960).
[14] For a review, see T. Suzuki, in *Lattice '92*, Proceedings of

the International Symposium, Amsterdam, the Netherlands, edited by J. Smit and P. van Baal [Nucl. Phys. B (Proc. Suppl.) **30**, 176 (1993)].

[15] P. Cea and L. Cosmai, in *Lattice '94*, Proceedings of the International Symposium, Bielefeld, Germany, edited by F. Karsch *et al.* [Nucl. Phys. B (Proc. Suppl.) **42** (1995)]; Phys. Lett. B **349**, 343 (1995).

[16] A. Di Giacomo, M. Maggiore, and Š. Olejnìk, Phys. Lett. B **236**, 199 (1990); Nucl. Phys. **B347**, 441 (1990).

[17] P. Cea and L. Cosmai, in *Lattice '92* [14], p. 572; Nuovo Cimiento A **107**, 541 (1994).

[18] A. Di Giacomo, Acta Phys. Pol. B **25**, 215 (1994).

[19] M. Campostrini, A. Di Giacomo, H. Panagopoulos, and E. Vicari, Nucl. Phys. **B329**, 683 (1990).

[20] M. Campostrini, A. Di Giacomo, M. Maggiore, H. Panagopoulos, E. Vicari, Phys. Lett. B **225**, 403 (1989).

[21] L. Del Debbio, A. Di Giacomo, and G. Paffuti, Phys. Lett. B **349**, 513 (1995); L. Del Debbio, A. Di Giacomo, G. Paffuti, and P. Pieri, in *Proceedings of the 27th International Conference on High Energy Physics*, Glasgow, Scotland, 1994, edited by P. J. Bussey and I. G. Knowles (IOP, London, 1995).

[22] V. Singh, D. A. Browne, and R. Haymaker, in *Lattice '92* [14], p. 568; Phys. Rev. D **47**, 1715 (1993).

[23] J. Fingberg, U. Heller, and F. Karsch, Nucl. Phys. **B392**, 493 (1993).

[24] V. Singh, D. A. Browne, and R. Haymaker, Phys. Lett. B **306**, 115 (1993).

[25] Y. Matsubara, S. Ejiri, and T. Suzuki, in *Lattice '93*, Proceedings of the International Symposium, Dallas, Texas, edited by T. Draper *et al.* [Nucl. Phys. B (Proc. Suppl.) **34**, 176 (1994)].

[26] T. A. De Grand and D. Toussaint, Phys. Rev. D **22**, 2478 (1980).

[27] See, for instance; M. Tinkham, *Introduction to Superconductivity* (McGraw-Hill, New York, 1975).

[28] L. Del Debbio, A. Di Giacomo, M. Maggiore, and Š. Olejnìk, Phys. Lett. B **267**, 254 (1991).

[29] For a thorough discussion of the overrelaxation algorithms for lattice field theories, see S. L. Adler, Phys. Rev. D **37**, 458 (1988).